# Combined Antennas for High-Power Ultrawideband Pulse Radiation

Yu.A. Andreev, Yu.I. Buyanov, V.I. Koshelev

*Institute of High Current Electronics SB RAS, 2/3 Akademichesky Ave., Tomsk, 634055, Russia,*
*Ph: (3822) 491-900, Fax:(3822) 492-410, E-mail: andreev@lhfe.hcei.tsc.ru*

**Abstract – The paper presents the analysis of factors influencing antenna frequency bandwidth. The ways of widening antennas bandwidth into low- and high- frequency ranges are shown. Design and characteristics of three combined ultrawideband antennas are described.**

## 1. Introduction

Creation of high-power ultrawideband radiation sources with a steering antenna array as a radiator is a promising direction of UWB radio electronics. Exacting requirements occasionally contradicting to each other are made to an element of such array. The element should be compact so that the distance between the antenna inputs (phase centers) will be not higher than the half of the exciting pulse spatial extension. A pattern should be unidirectional and radiation characteristics should be maximum close for possibly larger angles of deviation from the main maximum direction in the operating half-space. Besides, the antenna should have a passband essentially large for efficient radiation of exciting pulses.

## 2. Antenna frequency bandwidth

To evaluate the maximum admissible (theoretically) antenna passband, we'll use Fano theorem [1]. Relation between the relative matching band, load Q-factor and admissible voltage standing-wave ratio (VSWR) is expressed by the formula:

$$\frac{\omega_h - \omega_l}{\sqrt{\omega_h \omega_l}} = \frac{\pi}{Q[\ln(\mathrm{VSWR}+1) - \ln(\mathrm{VSWR}-1)]},$$

where $\omega_h$ and $\omega_l$ are the high and low boundary frequencies of the matching band.

Fig. 1 presents the load Q-factor versus the frequency overlapping factor $в = \omega_h/\omega_l$ for several values of VSWR.

To determine the antenna Q-factor, we'll use results of Ref. [2] presenting the analysis of energetic relations near the linear radiator, according to which the complete field energy in the near-field contains the following components:

а) energy being in a radiating state $W_\Sigma$;

б) reactive energy $W_r$;

в) bound energy $W_b$ participating in the mutual exchange between electrical and magnetic energies.

Energy store in the near-field is equal to the sum of reactive $W_r$ and bound $W_b$ energies. In case of a linear radiator that can be considered as a guide system for a current wave with the wave impedance $\rho_a$ and a propagation constant $\gamma$, the bound energy in its turn consists of the energy $W_{bc}$ stored in the current wave propagating along the radiator and of the energy $W_{b\Sigma}$ "radiated" into the region of imaginary angles.

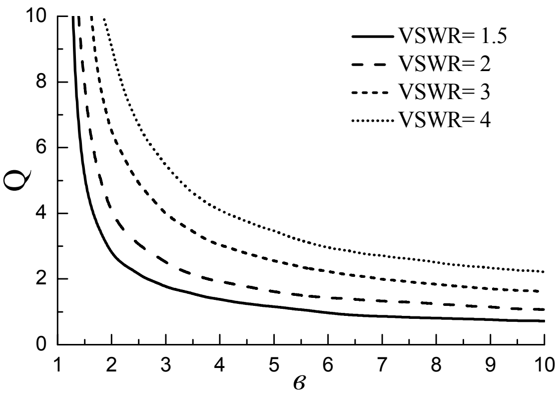


Fig. 1. Q-factor versus frequency overlapping for different VSWR.

The Q-factor of the linear radiator can be expressed through its characteristics (input impedance, propagation constant, and pattern) in the following way:

$$Q_a = Q_r + Q_{bc} + Q_{b\Sigma} = \frac{|X_a|}{R_a} + \frac{Re(\gamma)}{2Im(\gamma)} + \left( \frac{\int_{-\infty}^{\infty} |F(\xi)|^2 d\xi}{\int_{-k}^{k} |F(\xi)|^2 d\xi} - 1 \right).$$

The obtained ratio shows that the antenna Q-factor can be presented by the sum of partial Q-factors differently depending on the radiator parameters and allows determining what radiation parameters most essentially influence its matching band.

Fig. 2 presents frequency dependencies of $Q_{b\Sigma}$, $Q_{bc}$ and $Q_r$ of a 2L-length dipole with the wave impedance $\rho_a$ =500 Ohm (solid lines) and $\rho_a$ = 200 Ohm (dash lines). These results show that for expanding the short dipole matching band it is necessary first of all to decrease $Q_r$ and $Q_{bc}$. However, one fails to provide VSWR < 2 if L/λ < 0.2 and the ratio of the passband boundary frequencies is not higher than three since at L/λ > 0.6 the dipole pattern shape changes sharply.

Thus, passband expansion is possible owing to the matching band broadening towards the lower frequency region. For this purpose it is necessary to minimize $Q_r$. An efficient way to decrease $W_r$ store besides increase of transverse dimensions is combination of the near-field zones of the electric type radiator with magnetic type one.

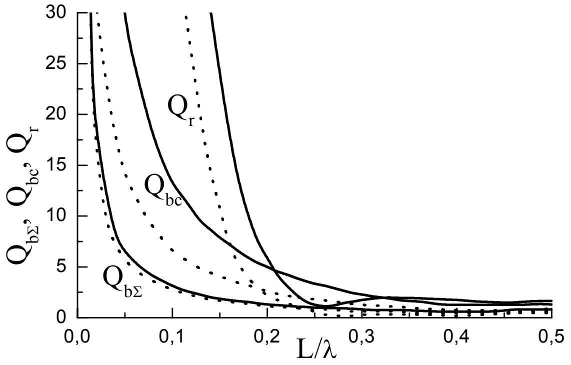


Fig. 2. Partial Q-factors of 2L length dipole versus L/λ.

As it is shown in Ref. [2], in the antennas presenting a combination of electrical and magnetic radiators (combined antennas), when definite amplitude-phase relations are provided it is possible not only to minimize $W_r$ but also to attenuate frequency dependence of $W_\Sigma$ that determines the real part of the input antenna impedance $R_a$. Besides, at the mutually orthogonal orientation of the electrical and magnetic radiators there appears a possibility to increase the directivity owing to the cardioid type pattern formation.

In real antennas one fails providing $W_r = 0$, therefore practically the low boundary of the matching band is achieved at $2L = \lambda/5 \div \lambda/6$ and further passband broadening is possible only towards the upper frequencies. For this purpose it is necessary to provide stabilization of the pattern maximum direction at the frequency change. The simplest way to stabilize the pattern maximum is that the dipole arms are placed at a certain angle $2\theta_0$ to each other (V-antenna). Fig. 3 presents calculated field patterns of the dipole with the wave impedance $\rho_a = 200$ Ohm with $2\theta_0=180°$ and of the V-antenna having the angle between the arms $2\theta_0=90°$. Presented results show that at $2L > \lambda$ and $100° > 2\theta_0 > 60°$ the pattern maximum direction is stabilized and the radiator directivity is even increased.

Hence, combination of a dipole and frame (or slot) allows broadening the passband towards the lower frequency region and making a dipole in the form of a V-antenna – towards the higher frequency region. At a corresponding choice of parameters of electrical and magnetic radiators the combined antenna passband can reach three octaves and more.

## 3. Combined antennas design

Fig. 4 presents variants of designs of high-power nanosecond pulse radiators.

The antennas A1 (Fig. 4a) and A2 (Fig. 4b) [2] can be considered as a combination of electrical and magnetic radiators. The third variant - antenna A3 (Fig. 4c) [3] can be considered as a combination of the electrical monopole *1*, active magnetic dipole *5*, *TEM*-horn *6,* and passive magnetic dipoles *7*. The antenna A3 can be considered as well as a combination of the *TEM*-horn *6*, active magnetic dipole *5* and passive magnetic dipoles *7*. An active dipole is excited by the conducting currents along the initial part of the electrical monopole *1*, along the surface of the plate *4* and the internal surface of the case-screen *2*. Passive magnetic dipoles are excited by the electromagnetic field. In the rear wall of the antennas there are connectors to connect the feeder with the wave impedance of 50 Ohm.

Overall dimensions of the antennas $L \cong c\tau/2$ (*c* is the velocity of light, τ is the bipolar pulse length in the transmission feeder). The height and the width of the antenna A3 are $h \le L$.

Antennas A1 optimized to radiate bipolar pulses of the length 4 (A14) and 3 ns (A13); antenna A2 optimized to radiate bipolar pulses of the length 2 ns (A22); antennas A3 optimized to radiate bipolar pulses of the length 3, 2 and 1 ns (A33, A32, A31) have been developed and investigated.

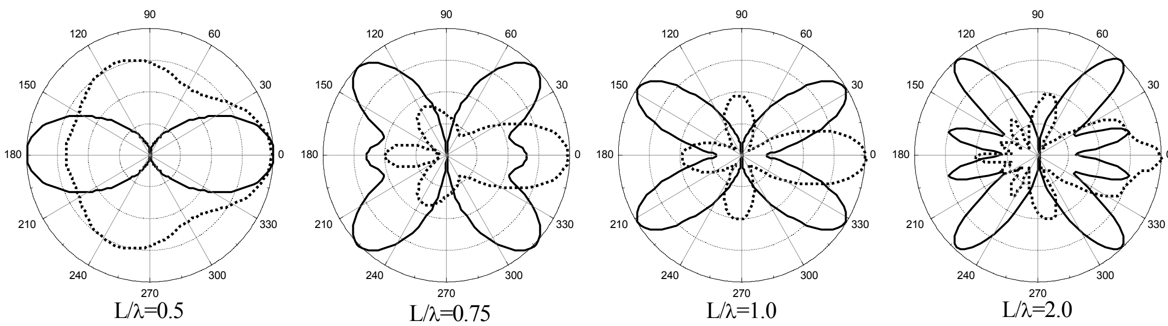


Fig. 3. Electrical dipole patterns: $2\theta_0 = 180°$ (solid lines), $2\theta_0 = 90°$ (dash lines).

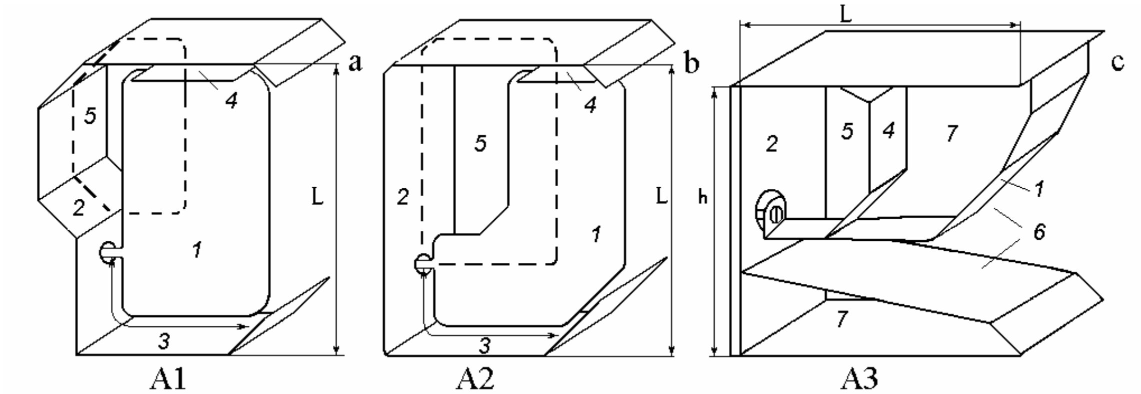


Fig. 4. Combined antennas geometry. *1* – electrical monopole, *2* – case, *3* – slot line, *4* – plate, *5* – active magnetic dipole, *6* – TEM-horn, *7* – passive magnetic dipole.

**4. Combined antenna characteristics in frequency domain**

Fig. 5a presents VSWR of the antenna A13 and the electrical monopole of this antenna, where an unfolded case (*2*, Fig. 4) of the A13 was used as a screen. Fig. 5b presents the analogous dependences for A22. As it is seen from Figs. 5a, b, the low boundary frequency of the matching band $f_l$ determined by the level of VSWR = 3 decreases for combined antennas.

To shift the antenna A32 $f_l$ towards the region of lower frequencies, the edges of the plates of the *TEM*-horn were connected with the antenna rear wall forming an active (upper) and passive (lower) magnetic dipoles. Additional antenna tuning is realized by partitioning of the upper magnetic dipole into two by means of the plate (*4*, Fig. 4c). Fig. 6a presents VSWR of the antenna A32 and of the *TEM*-horn of this antenna. It is seen that $f_l$ of the combined antenna A32 is shifted by 38% towards the lower frequencies relative to $f_l$ of the *TEM*-horn. Fig. 6b presents amplitude frequency response of the antenna A32 and of the *TEM*-horn of this antenna for the observation angle corresponding to φ, δ = 0°, where φ is the azimuth angle and δ is the elevation angle. The shift $f_l$ of the combined antenna A32 towards the lower frequencies relative to $f_l$ of the *TEM*-horn is seen as well. Besides, amplitude frequency response of the combined antenna has essentially more smooth

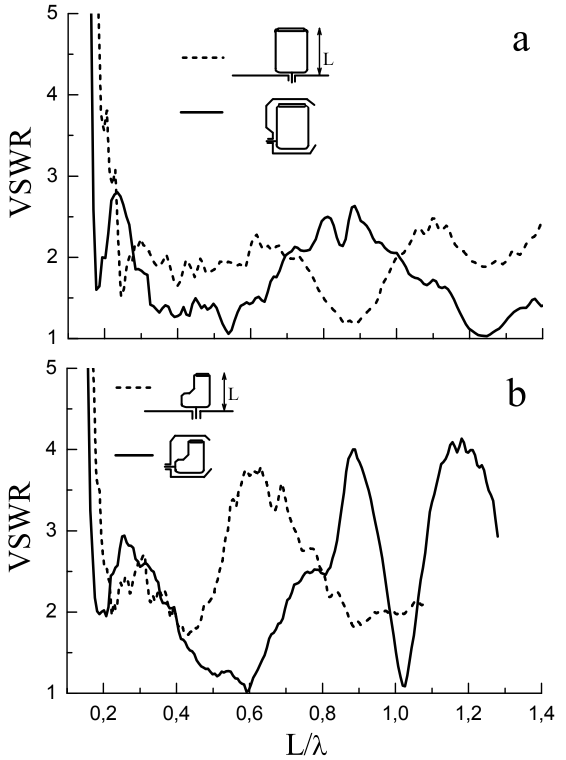


Fig. 5. VSWR of electrical monopol and A13 antenna (a), monopol and A22 antenna (b).

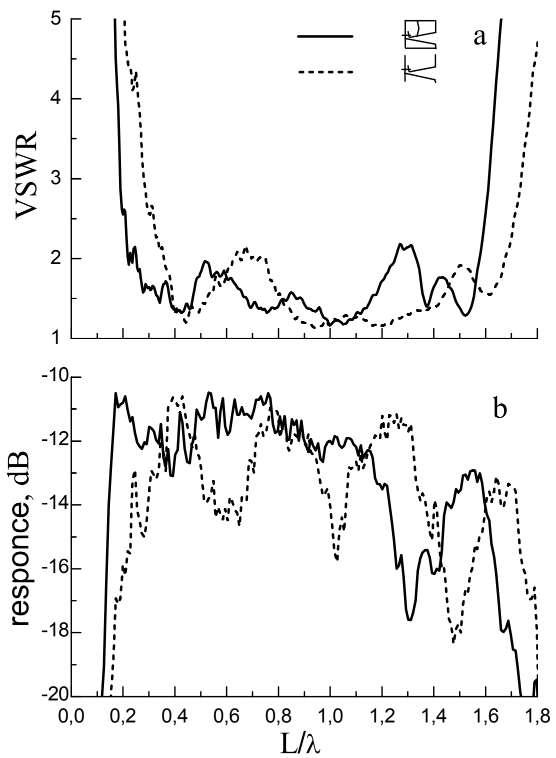


Fig. 6. VSWR (a) and amplitude frequency response (b) of TEM-horn and A32 antenna.

curve in comparison with the amplitude response of the *TEM*-horn. Depending on position of the plate *4,* characteristics of antennas A3 differ essentially [3].

The antennas passband can be determined as a frequency range in which the following conditions for low-distorted signal transmission are fulfilled: change of amplitude frequency response of the antenna relative the average value is in the limits of ±1.5 dB and deviation of the phase frequency response from linear one is in the limits of $\pm\pi/16$. Measurements were made for observation angles of 0°, ±30°, ±45° in the *E*- and *H*-planes.

Table 1 presents the data concerning the passband of combined antennas. It is seen that the passband of the antennas A3 is broadened in comparison with the antennas A1 and A2 for all observation angles. The passband is broadened towards the region of high frequencies due to application of the *TEM*-horn in the antenna A3.

**5. Combined antennas characteristics in time domain**

Investigation of antennas was carried out in the mode of supplying bipolar (BP) and monopolar (MP) voltage pulses to the antenna inputs.

Energetic efficiency of antennas was determined as

$$k_w = W_{rad}/W_{gen},$$

where $W_{rad}$ is the energy radiated by the antenna, $W_{gen}$ is the energy in the voltage pulse at the antenna input. Radiated energy was found experimentally as the difference of energy in the voltage pulse at the antenna input and energy in the pulse reflected from the antenna. Directivity factor $D_0$ was determined by the patterns of combined antennas in the main planes. When one knows voltage dependence on time at the antenna input, value $k_w$ of the antennas and spatial-temporal characteristics of antenna radiation, one can find antenna efficiency by the peak power

$$k_p = P_{rad}/P_{gen},$$

where $P_{rad}$ is the peak power value of the vertically polarized radiation and $P_{gen}$ is the peak power in the pulse at the antenna input.

Antenna efficiency by radiated field is determined from the relation

$$k_E = E_p R/U_p,$$

where $E_p$ is the electric field peak strength, R is the distance, $U_p$ is the voltage pulse peak value at the antenna input.

Comparative characteristics of combined antennas are presented in Table 2.

Table I. Combined antennas bandwidth

| Antenna name | φ, δ = 0° | φ = ±30°, δ = 0° | φ = ±45°, δ = 0° | φ = 0°, δ = 30° | φ = 0°, δ = 45° | φ = 0°, δ = -30° | φ = 0°, δ = -45° |
|---|---|---|---|---|---|---|---|
| A14 | 1.9 | 1.8 | 1.8 | 3 | 2.4 | 2 | 1.9 |
| A13 | 1.9 | 2 | 2.1 | 2 | 1.9 | 1.5 | 1.4 |
| A22 | 1.5 | 1.5 | 1.5 | 1.4 | 1.3 | 1.3 | 1.1 |
| A33 | 4.6 | 3.5 | 2.3 | 5.5 | 4 | 2.9 | 2.4 |
| A32 | 5.5 | 4.2 | 2.2 | 5.4 | 4.2 | 3.6 | 2.4 |
| A31 | 4.8 | 3.2 | 2.2 | 4.8 | 3.1 | 3.6 | 2.3 |

Table 2. Combined antennas characteristics

| Antenna name | $k_w$ | | $D_0$ | | $k_p$ | | Peak power pattern FWHM, degree | | | | $k_E$ | |
|---|---|---|---|---|---|---|---|---|---|---|---|---|
| | | | | | | | H-plane | | E-plane | | | |
| | MP | BP | MP | BP | MP | BP | MP | BP | MP | BP | MP | BP |
| A14 | 0.62 | 0.62 | 2.9 | 2.5 | 0.3 | 0.55 | 105 | 100 | 120 | 145 | 2 | 1.9 |
| A13 | 0.6 | 0.6 | 2.5 | 2.7 | 0.25 | 0.6 | 120 | 95 | 140 | 140 | 1.5 | 1.4 |
| A22 | 0.45 | 0.45 | 2 | 2.1 | 0.3 | 0.75 | 180 | 170 | 140 | 140 | 1.3 | 1.1 |
| A33 | 0.6 | 0.6 | 3.8 | 3.8 | 0.45 | 1.1 | 85 | 85 | 90 | 90 | 2.9 | 2.4 |
| A32 | 0.72 | 0.72 | 3.9 | 4.2 | 0.45 | 1 | 90 | 85 | 90 | 90 | 3.6 | 2.4 |
| A31 | 0.64 | 0.64 | 3.4 | 3.7 | 0.25 | 0.85 | 90 | 90 | 95 | 95 | 3.6 | 2.3 |

**References**


[1] R.M.Fano, Journal of the Franklin Institute, **249**, 57 (1950).

[2] V.I.Koshelev, Yu.I.Buyanov, B.M.Kovalchuk, Yu.A.Andreev, V.P.Belichenko, A.M.Efremov, V.V.Plisko, K.N.Sukhushin, V.A.Vizir, V.B.Zorin, Proc. SPIE**. 3158**, 209 (1997).

[3] V.I.Koshelev, Yu.I.Buyanov, Yu.A.Andreev, V.V.Plisko, K.N.Sukhushin, *in Proc. IEEE Pulsed Power Plasma Science Conf.*, V.2, 2001, pp.1661-1664.